British Biotechnology Journal
3(4): 524-544, 2013

SCIENCEDOMAIN *international*
www.sciencedomain.org

Dynamic Principle of Center of Mass in Human Walking

Yifang Fan[1*], Yubo Fan[2], Zhiyu Li[3], Mushtaq Loan[4] and Changsheng Lv[1]

[1]Center for Scientific Research, Guangzhou Institute of Physical Education, Guangzhou 510500, P.R. China.
[2]Key Laboratory for Biomechanics and Mechanobiology of Ministry of Education, School of Biological Science and Medical Engineering, Beihang University, Beijing 100191, P.R. China.
[3]College of Foreign Studies, Jinan University, Guangzhou 510632, P.R. China.
[4]International School, Jinan University, Guangzhou 510632, P.R. China.

Authors' contributions

This work was carried out in collaboration between all authors. Author Fan YF and Fan YB designed the study, performed the statistical analysis and wrote the protocol. Fan YF, Li ZY and Loan M managed the literature searches and wrote the first draft of the manuscript. Lv CS conducted the experiment of the study. All authors read and approved the final manuscript.

Research Article

Received 3rd May 2013
Accepted 19th July 2013
Published 10th August 2013

ABSTRACT

Assuming the ground reaction force of both feet to be the same in the same phase of a stride cycle, we establish the relationships between the time of initial foot contact and the ground reaction force, acceleration, velocity, displacement and average kinetic energy of center of mass. We employ the dispersion to analyze the effect of the time of the initial foot contact that imposes upon these physical quantities. We present results of an analytic and numerical calculation that studies the relationship between the time of initial foot contact and the ground reaction force of human gait and explores the dynamic principle of center of mass. Our study reveals that when the time of one foot's initial contact falls right in the middle of the other foot's stride cycle, these physical quantities reach extrema. An action function has been identified as the dispersion of the physical quantities and optimized analysis used to prove the least-action principle in gait. In addition to being very significant to the research domains such as clinical diagnosis, biped robot's gait control,

**Corresponding author: Email: tfyf@gipe.edu.cn;*

the exploration of this principle can simplify our understanding of the basic properties of gait.

Keywords: Gait; center of mass; forward dynamics method; least-action principle; musculoskeletal system diseases.

1. INTRODUCTION

Gait analysis plays an important role in exploring laws of human motion by gait parameters via biomechanical methods. Many studies have shown that gait parameters are significantly symmetric [1,2] and can be understood in terms of segmental kinematical and kinetic physical quantities, while walking. It has been shown, [3,4] that by developing gait parameters into evaluation indexes, one can assess the causal relationship between physical injury and gait ability, which in turn has been applied in rehabilitation therapy with success [3,5,6].

The essence of human center of mass (COM) motion is actually the periodical change which is under the effect of external forces such as, ground reaction force (GRF), gravity and resistance [7]. Previous studies indicate that the law of COM motion is a more reliable gait evaluation method [8]. The common features of the frequently-used gait indexes lie in the fact that normal human gait parameters have been regarded as the criteria to evaluate rehabilitation. However, the incomplete symmetry of human shape, coordinate and strength has formed the uniqueness of human gait [9]. This has brought difficulty to the establishment of standard gait parameter index. Consequently, exploring a principle that is relevant to gait parameters such as cycle time, cadence or stride length in a normal human gait has become essential to the study of gait biomechanics [10]. There are a number of issues we wish to explore in our calculation. An important question is whether the relationships between the GRF, velocity of COM, average kinetic energy and the time of initial foot contact (tIFC) in a stride cycle can be established. In particular we wish to examine if and to what extent such relationships explore the principle behind the gait characteristics. In the present work, we wish to advance an attempt towards an approach where the precision of the calculation reaches new levels.

By examining the GRF acted on the normal human gait (bare-footed), we establish the relationships between the GRF, velocity of COM, average kinetic energy and the tIFC in a stride cycle. In this contribution we present our recent results on kinetic regularities of COM. Another crucial issue in this attempt concerns the prediction of action in gait. Using analytic and numerical techniques, we shall identify the action in gait and explore the possibility of the least-action principle in gait [10]. The rest of the paper is organized as follows:

In Sec. II we describe our procedure to establish the relationships between the GRF and the tIFC and discuss the aspects of determination of the force distribution in anteroposterior, mediolateral and vertical directions. We address the problem of the force distribution in transverse, sagittal and frontal planes and optimization of dispersion of force. We present a description of the determination of working parameters, such as acceleration, velocity and displacement of COM and establish the relationships between the kinetic regularities and the tIFC in this section. We conclude this section by addressing the effect of the tIFC upon the average kinetic energy of COM. Our main results are presented and discussed in Sec. III. Finally, we present our conclusions in Sec. IV.

2. ANALYSIS STRATEGY - FORWARD DYNAMIC METHOD

2.1 The Effect of tIFC Upon GRF

The analysis of COM's dynamic characteristics to evaluate the gait features is rather non-trivial. The inverse dynamics method [8,11,12] has given mixed results with systematic and statistical errors as major sources of uncertainties in the analysis of COM dynamics characteristics [13]. An attempt to indicate the dynamic characteristics of the whole body COM by one particular segment of body will highly underestimate the results. The target of this work is a calculation that gives more precise estimates of dynamic measurements in question. We use forward dynamics method [14,15] to illustrate how tIFC determines the force distribution and establish a relationship between the tIFC and its force dispersion.

Since dynamic characteristics of COM in gait is governed by kinematics and kinetics of COM, therefore, for constant gravity, the analysis of force upon COM will compliment the analysis of GRF. Also, GRF is caused by the body segmental movement driven by the transarticular muscles and eventually by the contact of the foot to the ground, so one foot's GRF includes the vertical GRF, frontal friction and sagittal friction, i.e.

$$F(t) = F_x(t) + F_y(t) + F_z(t) \tag{1}$$

where $F(t)$ is refer to a function (GRF) dependent on time and $F_x(t)$, $F_y(t)$ and $F_z(t)$ represent the components in three directions, respectively. If $F_i^l(t)$ and $F_i^r(t)$ ($i=x,y,z$) represent both feet's sagittal and frontal frictions and vertical GRF, respectively, then the above equation shows a similarity of both feet's GRF distribution when expressed in biped gait features [10]. Consequently, we assume that in each stride cycle, the left and right foot have a geometrical approximation to the GRF curves in all three directions. This would imply that the GRF variations are only caused by the tIFC of both feet. Setting T as one foot's stride cycle time, the initial phase of one foot is equal to zero and that of the other foot to (i.e. tIFC), then corresponding to one foot's GRFs (for example left foot)

$$F_x^l(t) = F_x(t), F_y^l(t) = F_y(t), F_z^l(t) = F_z(t),$$

those of the other foot are

$$F_x^r(t) = F_x(t + t_o), F_y^r(t) = F_y(t + t_o), F_z^r(t) = F_z(t + t_o),$$

and Eq. 1 becomes

$$F(t, t_o) = F_x(t, t_o) + F_y(t, t_o) + F_z(t, t_o). \tag{2}$$

Since gait is a continuous and periodic movement, therefore while walking at steady speeds, $F(t,t_o)$ is the GRF when tIFC is to and the stride cycle t. If $F(t,t_o)=F(t+nT,t_o+nT)$ $(n=1,2,3\ldots)$ holds, then the GRF and gravity (*Weight*) in a stride cycle that act on the impulse of COM will follow the following equation:

$$I = I_x + I_y + I_z \equiv 0. \tag{3}$$

To calculate the impulse characteristics of each foot's GRF in gait when both feet have the same GRF, we analyze two phases of one foot's stride cycle. Let T_s and T_w represent the stance phase and swing phase, respectively, then in the anteroposterior direction, Eqs. 2 and 3 yield

$$\int_o^T F_x(t)dt = 0 \qquad and \qquad \int_o^T F_x(t)dt = \int_o^T F_x(t+t_o)dt.$$

Since $T=T_s+T_w$ and $\int_{T_s}^{T} F_x(t)dt = 0$, therefore

$$\int_0^{T_s} F_x(t)dt = \int_0^{T_s} F_x(t+t_o)dt = 0,$$

whereas in the mediolateral direction, we get

$$\int_0^{T_s} F_y(t)dt = \int_0^{T_s} F_y(t+t_o)dt = 0.$$

On the other hand, the calculated contribution in the vertical direction gives

$$\int_0^{T} F_z(t)dt = \int_0^{T} F_z(t+t_o)dt = \frac{1}{2}Weight$$

The above equations give the impulse characteristics of each foot's GRF in gait.

2.2 Dispersion of GRF

To analyze the dynamics that emerge in the GRF distribution at $t_o=0,T/2$ and T, we bring forward the concept of dispersion of GRF. If σ_i ($i=x,y,z$) and $\overline{F}_i$ denote the GRF dispersions and average values of GRF in three directions, then the corresponding correlation between the force dispersion and average GRF can be written as

$$\sigma(t_o) = \sqrt{\sum_{t=0}^{T}\left(F_i\left(t,t_o\right) - \overline{F}_i\left(t_o\right)\right)^2 \Big/ T\sum_{t=0}^{T}1}, \tag{4}$$

where $F_i(t,t_o)$ is the same as that in Eq. 2 and $\sum_1^T 1$ is the number of Δt within the range $[0,T]$. For sequential values of t_o within the range $[0,T]$, we calculate the values of σ_i and use them to evaluate the effect of tIFC upon GRF, velocity, position and kinetic energy of COM. We use the average value of GRF from 20 subjects to check the reliability and accuracy of this method. This signature is confirmed in Sec. III of this study.

2.3 Regularities of Velocity and Displacement of COM

By defining F_x to oscillate around the zero [16,17] (i.e. $\frac{1}{T_{step}}\int_0^{T_{step}} F_x^{feet}(t)dt = 0$, or $\frac{1}{T_s}\int_0^{T_s} F_x^{foot}(t)dt = 0$) and F_z to oscillate around a force value equal to the subject's body weight [16,17] (i.e. $\frac{1}{T}\int_0^{T} F_z^{feet}(t)dt = 1$, or $\frac{1}{T_{step}}\int_0^{T_{step}} F_z^{feet}(t)dt = 1$, or $\frac{2}{T_{step}}\int_0^{T_{step}} F_z^{foot}(t)dt = 1$), anteroposterior and vertical kinematic quantities of COM can be calculated, but not those of the mediolateral direction. So we define Fy to oscillate around the zero (i.e. $\frac{1}{T}\int_0^{T} F_y^{feet}(t)dt = 0$) in a stride cycle.

It is known that the absolute velocity of COM is equal to relative velocity plus convected velocity. The convected velocity refers to the walking speed. The acceleration of COM determines its relative velocity, not relating to the convected velocity. This means that when a stride cycle begins, the initial velocity of COM must be known. The definition that the average vertical velocity of COM over a step is zero [11,16,18] cannot come up with the initial velocity of COM in mediolateral direction. Therefore, we define an integration constant for every direction by requiring the average COM velocity over a stride cycle to be zero.

To sum up, the effect of tIFC upon the dynamic quantities of COM discussed in our paper corresponds with the following condition equations:

$$\frac{1}{T_{step}}\int_0^{T_{step}} F_x^{feet}(t)dt = 0, \frac{1}{T}\int_0^{T} F_y^{feet}(t)dt = 0, \frac{1}{T_{step}}\int_0^{T_{step}} F_z^{feet}(t)dt = 1 \quad (5)$$

Ground reaction force[1] is the result of body segments action on the ground via foot and determines the kinematical regularities such as acceleration, velocity and displacement of human body COM. Knowing the GRF and weight, the acceleration of COM at a given instant in a stride cycle using Eq. 2 can be written as

$$a(t,t_o) = \left(F(t,t_o) - 1\right)g \quad (6)$$

where g is the acceleration of gravity and weight mg is standardized to 1 by condition Eq. 5. Expressing the acceleration of COM in component form, Eqs. 1 and 6 reveal that the tIFC and GRF have the same effect on the acceleration of COM.

The absolute motion of human COM relative to absolute inertia reference frame is composed of convected motion and relative motion. Following Kokshenev [7], we define gait in accordance with motion in Eq. 3, as "walking at steady speeds", thus we regard the

[1] *We assume a constant gravity and a negligible air resistance.*

convected motion a constant parameter. Using Eq. 6 at tIFC = t_o, the COM velocity in a stride cycle is given by

$$v(t,t_o) = \int_0^t a(t,t_o)dt + v_o(t_o), \tag{7}$$

where $v_0(t_o)$ is the initial velocity of COM in relative motion at the beginning of a stride cycle. It seems that we cannot confirm the magnitude of $v(t,t_o)$ in Eq. 7 by kinetic method (since everyone's gait speed is different). However, the distinct feature is that once GRF and tIFC are determined and when it observes the motion in Eq. 3, $v_0(t_o)$ must have a unique solution. We can then establish the relationship between the initial velocity and acceleration in relative motion in a stride cycle

$$v_0(t_o) = -\sum_{\lambda=1}^{T}\int_0^{\lambda} a(t,t_o)dt. \tag{8}$$

Eq. 7 reveals that $v(T,t_o)=v(t_o)$, which implies that the cycle of velocity of COM is in accordance of $v(T+nT,t_o+nT)$ $(n=1,2\ldots)$, that is to say, the end of one stride cycle marks the beginning of the next stride cycle. This explains the periodical characteristics of velocity of COM in gait. What needs to be further illustrated is that the initial velocity calculated using Eq. 8 suggests that at the beginning of a stride cycle, the body is in the state of steady speeds. From Eqs. 6 and 8 we conclude that tIFC has determined the initial velocity in relative motion, which has nothing to do with the convected velocity.

Just like the velocity of COM, displacement of COM also involves absolute, convected and relative displacements. We define the COM initial displacement in relative motion of different tIFC as $s_0(t_o)$. Using Eq. 7, the displacement of COM in relative motion at any moment has the following form:

$$s(t,t_o) = \int_0^t v(t,t_o)dt + s_o(t_o), \tag{9}$$

and the correlation between the initial displacement of COM and velocity of COM in relative motion in a stride cycle can be written as

$$s_0(t_o) = -\sum_{\lambda=1}^{T}\int_0^{\lambda} v(t,t_o)dt. \tag{10}$$

Similar to the behavior of the initial velocity in relative motion, we verified that the initial displacement seems to be independent of gait velocity, cadence and stride length.

2.4 Average Kinetic Energy

Nature has always minimized certain important quantities when a physical process takes place [19]. Bipedal walking has enabled the continuous evolution of human gait [20] and eventually it has brought about the optimized gait [21] and thus become a behavioral trait. In this behavior, the force, acceleration and velocity all have their minimal values when $t_o = \frac{1}{2}T$. To understand the physical significance of these gait dynamic characteristics we explore the issue of energy consumption. In gait, human segment movement is a

combination of agonist, antagonist and synergist. The movements such as stretch or flexure all consume mechanical energy. On the other hand, $E_k \geq 0$ in COM kinetic energy, $\sum_1^T E_k(t) \geq 0$ in total kinetic energy and $\overline{E}_k(t) \geq 0$ in average kinetic energy in a stride cycle, whereas the corresponding potential energy counterparts are zero respectively. The weight being normalized, using the COM kinetic energy in relative motion, the description of mechanical energy consumption in gait simplifies to

$$E_k(t,t_o) = \frac{1}{2} v^2(t,t_o), \tag{11}$$

and can be easily resolved in component form. Knowing E_i *(i=x,y,z)*, we can set up the relationships between tIFC and COM kinetic energy by defining t and t_o in the interval [*0,T*].

2.5 Experimental Details

When walking, to use the force plate(s) to collect GRF has been widely accepted [11,16,18,22-24]. One force plate can measure one foot's GRF. But it is difficult to distinguish the initial stride time when GRFs of many steps are measured by one force plate [17] that has a long platform (e. g. 3 meters). When two separate force plates [8,18] are used to measure the GRFs of one step, it is still difficult to tell the end of the step time[2]. As a result, in our experiment, three separate force plates were used [23].

The experimental measurements were carried out by the following set of equipment: Simi Motion 7.0 Three-Dimensional Movement Analysis System; three Kistler 40×60 (cm^2) force plates; force plate frequency: 2000Hz, with a systematic uncertainty of ±1%. The assembled force plate position was fixed by gradienter to ensure the force plates were on the same plane. The measurements were taken at the sample frequency of 1000Hz. Before each measurement, the equipment was examined and returned to zero-position. GRF data were filtered with a cutoff frequency of 100Hz. The instants of touchdown and takeoff from the force plate were defined as when the vertical GRF first rose above 5N (touchdown) and reduced to 5N (takeoff).

Twenty female subjects agreed to participate in the research and signed an informed consent form. The subjects were with mean age 20.63±0.76 years, mean height 163.12±3.72 cm and mean weight 45.74±3.30 kg. A few trials of each level gait item were administered to subjects as they ambulated on instrumented positions.

Before the test, all the subjects were thoroughly briefed about the procedures and matters needing attention so that they all understood the purpose and the requirements of the test. Each subject's medical history was inquired so as to exclude subjects with diseases such as pathological change, deformity or injury to make sure that their physical conditions could meet the requirements of the test. When measuring their gaits, we started from the subjects' standing position, bare-footed (both feet disinfected by 75% of ethanol). A pre-test was to guarantee that after they walked three steps, the subjects stepped on the platform and to make sure that each force plate can measure one foot's stance phase data separately. When the subject's gait was found to be quite abnormal, for example, it was obviously

[2]*When one foot steps on the first platform, there is no datum for the GRF of the other foot. When the other foot steps on the second platform, the timing for a "step" begins and the GRFs of both feet can be obtained. When one "step" finishes, the foot that steps on the first platform should step on a third platform. Then the time needed for one "step" is obtained.*

discontinuous, she would be asked to perform again so that the recorded data could meet the requirements of the test.

Based on the fact that the vertical GRF in gait is apparently greater than the GRFs of the anteroposterior or mediolateral direction, we take the signal of vertical GRF to identify the instants of initial foot contact and of terminal stance. The gait we study is walking at steady speeds; therefore, we de-noise the signals of the platform and examine the test signals to meet the requirements in the predetermined accuracy range. We rate the gait cycle time by percentage, normalize the weight and standardize the GRF from three directions. We count on average of the processed data of 20 subjects' three-direction GRF from individual stride cycle to conduct our research.

2.6 Ethic Statement

The study received approval from the Ethical Committee of Guangzhou Institute of Physical Education. The subject provided fully informed consent to participate in this study by signing a written consent form.

3. RESULTS AND DISCUSSION

3.1 Spatial GRF, COM Velocity and Displacement

To explore the spatial GRF, we examine Eq. 2 by using the GRF numeric of 20 subjects. Fig. 1 collects and displays the results of anteroposterior, mediolateral and vertical GRF.

The processing of data collected from force plate includes standardization of time and standardization of GRF. When doing the latter, gravity acceleration [7,17] or weight/gravity [24] is usually employed. No matter which method is employed, the calculation of kinematic quantity would be the same. But to standardize GRF by the gravity acceleration [17] or not to standardize GRF [18,22] is inappropriate. For example, the comparability of GRF of different subjects might be low. The components of GRF are standardized by condition Eq. 5 and stride cycle time is rated by percentage. Fig. 1.

Fig. 1A - C shows that tIFC has an effect upon the GRF in three directions. Using three sets of component data from GRF of the subject's gait, we obtain curved surface effective plots and the quantitative relationship between tIFC and GRF resultant forces on three planes. Fig. 1D - F indicates that no matter what changes t_o undergoes, GRF resultant forces in these three planes remain to be closed curves. This significantly compliments and confirms the dynamics behind Eq. 3, i.e., when the distribution of one foot's GRF is determined and both feet's GRFs remain the same, the momentum of COM always remains unaffected.

Fig. 1D - F also reveals the geometrical characteristics of the plane resultant force. In the transverse plane, when $t_o = 0, T$, the gait becomes a jump and its frontal resultant force becomes a straight line. The resultant force changes into a symmetrical butterfly about F_x, which could imply a possible transformation at $t_o = \frac{1}{2}T$. In the sagittal plane, when $t_o = 0, T$, the resultant force F_{xz} forms the longest closed curve (the length of which is calculated by $\oint F_{xz}(t, t_o) dF_x dF_z$) and more or less shortest at $t_o = \frac{1}{2}T$. In the frontal plane, the resultant

force develops into a straight line at t_o=*0,T*. The resultant force becomes a symmetrical butterfly about F_z at $t_o = \frac{1}{2}T$.

Having developed the relationship between tIFC and GRF's resultant force in three planes, we calculate the GRF dispersion in three directions using Eq. 4. To confirm the results beyond doubt, we identify the GRF dispersion by analyzing the effective plots shown in Fig. 1G - I. It is clear from the plots that at $t_o = \frac{1}{2}T$, σ_x has its maximum value at the bottom region of "W" shape, σ_y has a global maxima and σ_z a global minima. Using the numerical values, min (σ_x) =0.0695, max (σ_x) =0.1319, min (σ_y) =0.0000, max (σ_y) =0.0355, min (σ_z) =0.1086 and max (σ_z) =0.9144, of GRF dispersion obtained in this case study, we find that the largest differences between the maximal and minimal values are 0.0624, 0.0355 and 0.8058, respectively. This means that the dominant effect to the global GRF is the vertical GRF. The minimal GRF dispersion in vertical direction occurs at $t_o = \frac{1}{2}T$. The analysis of the distribution of GRF in three directions indicates that when $t_o = \frac{1}{2}T$, the anteroposterior and vertical dispersions of GRF are almost the least and the mediolateral one is the largest. The closed curve shaped by the two components in the sagittal plane seems to be the shortest. The GRF resultant force on the transverse and sagittal plane is shown as symmetric butterfly.

Turning our attention towards the kinematical regularities, we plot the effect of tIFC on COM velocity in Fig. 2A - C. We can see two plates in the left panel, which emerge at the two extremes of tIFC rated by percentage forming a concave region around tIFC whereas the velocity describes a convex region around tIFC. The COM velocity in the vertical direction indicates that tIFC entails the vertical velocity of COM to have a distribution of tIFC in the form of a saddle. In order to further understand the effect of tIFC exerting on the velocity of COM, we analyze the variations of the velocity of COM in three planes in Fig. 2D - F.

Looking at Fig. 2D - F, we notice that in the transverse plane, the direction of COM velocity is a straight line at t_o=*0,T* and the plane velocity becomes a symmetrical closed curve about v_x axis at $t_o = \frac{1}{2}T$. In the sagittal plane the closed curve formed by the plane velocity is the longest (the length of the closed curve is calculated by $\iint v(t,t_o)dv_x dv_z$ at t_o=*0,T*, and is shorter (not the shortest) at t_o=*0,T*. In the frontal plane, when t_o=*0,T*, the velocity becomes a straight line and the resultant velocity becomes a symmetrical closed curve about v_x axis at t_o=*0,T*. Having obtained the estimated value of COM velocity, we are ready to set up the dispersion of relationship between tIFC and COM velocity (as shown in Fig. 2G - I) using Eq. 4. We notice that at $t_o = \frac{1}{2}T$, σ_x and σ_y have the global minima and σ_z has the global maxima. The estimates, min (σ_x) =0.0541, max (σ_x) =0.1652, min (σ_y) =0.0000, max (σ_y) =0.0510, min (σ_z) =0.0549 and max (σ_z) =1.3502 in our case study, result in largest differences of maximal and minimal values of 0.1111, 0.0510, and 1.2953 respectively. This means that the dominant effect upon COM velocity lies in the vertical and anteroposterior direction, where the dispersions have the minimal values at $t_o = \frac{1}{2}T$.

The kinematical regularity of the displacement of COM in three directions is shown in Fig. 3A - C. The estimated values of the COM displacement components are used to evaluate the values and directions of COM displacement in three planes. We see a geometric distribution of convex corners indicating that tIFC changes the position of COM in anteroposterior direction. The bimodal plot indicates the complexity of vertical direction exerted by tIFC to the position of COM. To further analyze the effect of tIFC upon the position of COM, we explore the changes of COM positions from three planes which are displayed in Fig. 3D - F.

These effective plots show that in the transverse plane the COM displacement is a straight line at $t_o=0,T$. On the other hand, a closed curve is formed by s_x and s_y and is symmetric about s_x axis at $t_o = \frac{1}{2}T$. In the sagittal plane, when $t_o=0,T$, the closed curve shaped by the sagittal displacement is the longest (the length of the closed curve is calculated by $\iint s(t,t_o)ds_x ds_z$; when $t_o = \frac{1}{2}T$, the curve is rather shorter (but not the shortest). In the frontal plane the frontal displacement becomes a straight line at $t_o=0,T$ and a symmetric closed curve about s_y axis at $t_o = \frac{1}{2}T$.

Using the numerical values, $\min(\sigma_x)$=0.0042, $\max(\sigma_x)$=0.0252, $\min(\sigma_y)$=0.0000, $\max(\sigma_y)$=0.0081, $\min(\sigma_z)$=0.0039 and $\max(\sigma_z)$=0.2147, obtained in this case study, we find that of the GRF dispersion σ_x and σ_y have a global minima and σ_z has a global maxima at around $t_o = \frac{1}{2}T$, again resulting in largest differences between the minimal and maximal values with a magnitude of the order 0.0210, 0.0081 and 0.2108, respectively. This implies that the greatest effect to COM displacement comes from components in vertical and anteroposterior direction while the minimal dispersion of displacement in the vertical and anteroposterior direction emerges at $t_o = \frac{1}{2}T$ (Fig. 3G - I).

Accordingly, at $t_o = \frac{1}{2}T$, COM velocity in relative motion presents its symmetric closed curve in transverse and frontal plane and the curve length in the sagittal plane is approximately the minimal. In a stride cycle, the dispersion of COM velocity in relative motion has the global minima in the anteroposterior and vertical direction while the global maximal value in the mediolateral direction. The effect of tIFC upon the COM velocity and displacement does not depend on gait velocity, cadence or stride length whereas the effect of the tIFC upon COM acceleration is in accordance with the effect it exerts upon the GRF. The COM acceleration and GRF show more or less identical behavior. As is clear from Fig. 4 that at half stride cycle ($t=T/2$), the dispersion of GRF and COM kinematics are minimum. In comparison to GRF and COM velocity, the COM displacement shows a sharp dip with least minimum.

3.2 Anteroposterior, Mediolateral and Vertical Average Kinetic Energies

We show the fitted COM kinetic energies as a function of stride cycle in anteroposterior, mediolateral and vertical channels in Fig. 5A - C together with corresponding transverse, sagittal and frontal energies in three planes. Fig. 5D - F indicates that tIFC makes COM average kinetic energy the global minima in anteroposterior and mediolateral direction while that in the mediolateral direction a global maxima at $t_o = \frac{1}{2}T$. Comparing the relationship

between the tIFC's velocity of COM and the position of COM, tIFC contributes a symmetric distribution of kinetic energy of COM. Since $\min(E_x(t,t_o))>\max(E_y(t,t_o))$ and $\max(E_y(t,t_o))<\min(E_z(t,t_o))$, the anteroposterior and vertical average kinetic energies determine the COM average kinetic energy.

When tIFC falls at 20%, 50%, 60% and 100% of a stride cycle, the kinetic energy of COM in three planes varies rather considerably. In the transverse and frontal planes, the effect is similar whereas that in the sagittal plane undergoes a non-trivial change. We apply the dispersion of kinetic energy of COM to evaluate this effect. We notice, from Fig. 5G - J, that COM average kinetic energy is minimum at $t_o = \frac{1}{2}T$, which implies a minima for the COM mechanical energy consumption and signatures the physical significance of gait.

3.3 Approximation of GRF

The premise of an optimal analysis is to set up a target function. According to Cavagna's data [25], an approximation equation of both feet's GRFs in vertical and anteroposterior direction is set up [7]. Riener standardized the GRF components [24]. We use condition equations to standardize one foot's GRF component. According to our data (these results are consistent with Ref. [22] and Ref. [24]), we establish an approximation equation of one foot's GRF components:

$$\begin{cases} F_x(t) = a_1 \sin(a_2 \exp(a_3 \dfrac{t}{T_s}) \dfrac{t\pi}{T_s}) \\ F_y(t) = b_1 \exp(\sin(\dfrac{t\pi}{T_s})) + b_2 \exp(\cos(b_3 \dfrac{t\pi}{T_s})) + b_4 \\ F_z(t) = c_1 \exp(\sin(\dfrac{t\pi}{T_s} + c_2)) + c_3 \exp(\cos(c_4 \dfrac{t\pi}{T_s} + c_2)) + c_5 \end{cases} \quad (12)$$

where a_1 - a_3, b_1 - b_4, c_1 - c_5 are constants.

Fig. 6 is the result from adjusting the parameters (according to condition Eq. 5) in Eq. 12. Eq. 12 can certainly reflect the characteristics of one foot's GRF, but to discuss the effect of tIFC upon the dynamic quantity of COM, it is necessary to set up a target function of GRF resultant force. As a result, it is necessary to further simplify the equation.

The idea of inverted-pendulum walk [21,25-27] is widely accepted. Using $c\sin(\pi \frac{t}{T_s})$ to simulate the vertical GRF corresponds with the law of motion of COM when gait is simplified as an inverted pendulum. Let $c\sin(\pi \frac{t}{T_s})$ stand for the vertical GRF of one foot's stance and $c\sin(\pi \frac{t}{T_s})\sin(\pi \frac{t+t_o}{T_s}) + d$ (where d is a constant that meets the condition Eq. 5) for GRF of double-support stance. According to Eqs. 6 - 10, the result is shown as follows.

Fig. 7 shows that though difference exists between the law of motion of COM simplified by the approximation function of GRF and that of the real experiments, the effect of tIFC upon the motion of COM by simplified GRF function is in fact consistent with that of the real world. Both come to the same conclusion that when $t_o = \frac{1}{2}T$, the change range of displacement of

COM is the smallest. This is also true to the vertical acceleration and displacement. It can thus be concluded that the method to use the simplified GRF function to analyze the effect of tIFC upon the dynamic quantity of COM is feasible.

3.4 Least-Action Principle in Gait

The intriguing question arises from the above discussion if there is a symmetry or a physical principle that is hidden in the phenomenon that makes the COM kinetic energy to reach its extremum at $t_o = \frac{1}{2}T$. In order to explore this issue, we pursue the technique of optimizing the dispersion objective function [10]

$$\begin{aligned}\min \psi(t_o) &= \sum_1^T \left(F(t) + F(t+t_o) - \overline{F}(t_o)\right)^2 \\ &= \sum_1^T F(t)^2 + \sum_1^T F(t+t_o)^2 + 2\sum_1^T F(t)F(t+t_o) - 2\sum_1^T \left(F(t) + F(t+t_o)\right) + \left(\overline{F}(t_o)\right)^2 \sum_1^T 1 \end{aligned} \quad (13)$$

The action of GRF and gravity are the reasons for human COM motion changes. Let's first analyze the GRF. The average value of the resultant force in the anteroposterior and mediolateral direction $\overline{F}_x(t_o)$ and $\overline{F}_y(t_o)$ is zero and in the vertical direction $\overline{F}_z(t_o)$ is one (when the weight has been normalized). Therefore, for a known gait, $\sum_1^T \left(F_x(t)\right)^2$, $\sum_1^T \left(F_y(t)\right)^2$, $\sum_1^T \left(F_z(t)\right)^2$, $\sum_1^T \left(F_x(t+t_o)\right)^2$, $\sum_1^T \left(F_y(t+t_o)\right)^2$ and $\sum_1^T \left(F_z(t+t_o)\right)^2$ are all constants and Eq. 13 simplifies the dispersion optimization to

$$\begin{cases} \min \psi F_x(t_o) = \sum_1^T F_x(t)F_x(t+t_o) \\ \max \psi F_y(t_o) = -\sum_1^T F_y(t)F_y(t+t_o) \\ \min \psi F_z(t_o) = \sum_1^T F_z(t)F_z(t+t_o) \end{cases} \quad (14)$$

Through Eq. 12, pulse periodic GRF is acted upon foot. The vertical GRF of one foot presents a double-hump shape, but when studying the effect of the tIFC to the vertical GRF of both feet, we can make an additional simplification to the GRF function. We may use segment trigonometric functions and exponential functions to simplify it. That is to say, we simplify the GRF in three directions as

$$F_x(t) = a\sin\left(2\pi \tfrac{t}{T_s}\right), F_y(t) = b\sin\left(\pi \tfrac{t}{T_s}\right), F_z(t) = c\sin\left(\pi \tfrac{t}{T_s}\right)$$

where *a, b, c* stand for the GRF after normalization in three directions. For a small enough test frequency, the Eq. 14 transforms to

$$\begin{cases} \min \psi F_x(t_o) = A\int_0^{T_s} \sin\left(2\pi \dfrac{t}{T_s}\right)\sin\left(2\pi \dfrac{t+t_o}{T_s}\right)dt \\ \max \psi F_y(t_o) = -B\int_0^{T_s} \sin\left(\pi \dfrac{t}{T_s}\right)\sin\left(\pi \dfrac{t+t_o}{T_s}\right)dt \\ \min \psi F_z(t_o) = C\int_0^{T_s} \sin\left(\pi \dfrac{t}{T_s}\right)\sin\left(\pi \dfrac{t+t_o}{T_s}\right)dt \end{cases} \quad (15)$$

Let's take vertical GRF in Eq. 15 as an example. In order to get the antiderivative of the integrand of integral variable t, we detach t and to of trigonometric function to obtain

$$\int_0^{T_s} \sin\left(\pi \frac{t}{T_s}\right)\sin\left(\pi \frac{t+t_o}{T_s}\right)dt = \int_0^{T_s}\left(\sin^2\left(\frac{t\pi}{T_s}\right)\cos\left(\frac{t\pi}{T_s}\right) + \sin\left(\frac{t\pi}{T_s}\right)\cos\left(\frac{t\pi}{T_s}\right)\sin\left(\frac{t_o\pi}{T_s}\right)\right)dt \quad (16)$$

Now we can transform Eq. 16 into the integral of integral variable t while regarding the GRF as segment function. The transformation reduces the pulse periodic GRF functions into three piecewise functions at three intervals[3]: $[0, T_w]$, $[T_w, T_s]$ and $[T_s, T]$ which, to the confirmed GRF, *a, b, c* are constants and *A, B, C* (related to *a, b, c*) are also constants, yields the following form of vertical GRF:

$$\min \psi F_z(t_o) = C\begin{cases} \frac{1}{2}\sin(\pi\frac{t_o}{T_s}) - (\frac{t_o - T_s}{2T_s}\pi)\cos(\pi\frac{t_o}{T_s}), & 0 \le t_o \le T_w \\ \frac{1}{2}\sin(\pi\frac{t_o}{T_s}) - (\frac{t_o - T_s}{2T_s}\pi)\cos(\pi\frac{t_o}{T_s}) + \frac{1}{2}\sin(\frac{t_o - T_w}{T_s}\pi) - (\frac{t_o - T_w}{2T_s}\pi)\cos(\frac{t_o - T_w}{T_s}\pi), & T_w \le t_o \le T_s \\ \frac{1}{2}\sin(\frac{t_o - T_w}{T_s}\pi) - (\frac{t_o - T_w}{2T_s}\pi)\cos(\frac{t_o - T_w}{T_s}\pi), & T_s \le t_o \le T \end{cases} \quad (17)$$

The contribution

$$\left(\frac{t_o - T_s}{2T_s}\pi\right)\sin\left(\pi\frac{t_o}{T_s}\right) = 0$$

in the interval $[0, T_w]$, thus gives $t_o = 0$, which in turn yields (from Eq. 17) a maxima ($= \frac{C\pi}{2}$). On the other hand, the contribution

$$\left(\frac{t_o - T_s}{2T_s}\pi\right)\sin\left(\pi\frac{t_o}{T_s}\right) + \left(\frac{t_o - T_w}{2T_s}\pi\right)\sin\left(\pi\frac{t_o - T_w}{T_s}\right) = 0$$

in $[T_w, T_s]$ gives the solution $T_s - t_o = t_o - T_w$ which yields

$$C\left(\cos\left(\pi\frac{T_w}{2T_s}\right) - \left(\frac{T_s - T_w}{2T_s}\pi\right)\sin\left(\pi\frac{T_w}{2T_s}\right)\right)$$

[3] *While walking* $T_s + T_w = T$ *and* $T_s > T_w > 0$

(a minima). Similarly, we obtain a maximum value $\frac{C\pi}{2}$ in [T_s,T].

Following the above procedure, it is verified (from Eq. 15) that at t_o=$T/2$ the dispersion of GRF in the anteroposterior direction attains a minima of

$$A\left(\left(\frac{T_s-T_w}{T_s}\pi\right)\cos\left(\pi\frac{T_w}{T_s}\right)-\sin\left(\pi\frac{T_w}{T_s}\right)\right)$$

and a maxima of

$$B\left(\left(\frac{T_s-T_w}{2T_s}\pi\right)\sin\left(\pi\frac{T_w}{2T_s}\right)-\cos\left(\pi\frac{T_w}{2T_s}\right)\right)$$

in the mediolateral direction. Since, in gait, $A>B>C$, the sum of dispersions in three directions is minimal at $t_o=\frac{1}{2}T$. This confirms our results shown in Figs. 4D - F and 5J. Similarly, the dispersion of COM acceleration, dispersion of COM velocity and the COM mechanical energy consumption are all the minimal at $t_o=\frac{1}{2}T$. This phenomenon is independent of the physiological factors such as height, weight and gait parameters [10].

4. APPLICATION

Clinically, musculoskeletal system diseases can lead to the patients' asymmetrical gait parameters while walking. How would the musculoskeletal system patients perform from the perspective of dynamics of COM? We selected patients who recovered from hemiarthroplasty, achilles tendon rupture and rheumatoid arthritis and analyzed their kinematic characteristics of COM. Fig. 8.

Fig. 8 shows that when healthy young adults are walking, the curves of acceleration, velocity and displacement of their consecutive steps are basically consistent and symmetrical, but the musculoskeletal system diseases can damage this symmetry. Specifically, the left and right peak value of acceleration is not consistent; the velocity peak value is not consistent with the time when the peak value emerges; and neither is the displacement value consistent with the time when the peak value emerges. This indicates that musculoskeletal system diseases damage the symmetry of motion system, which can be reflected by the kinematics of COM.

The limitation of this research: our theoretical conclusion is based upon symmetrical method but not biomechanical hypothesis, which might bring risk to practical application. Also, our subjects are all females and the sample size is not very large, which may not be sufficient for application.

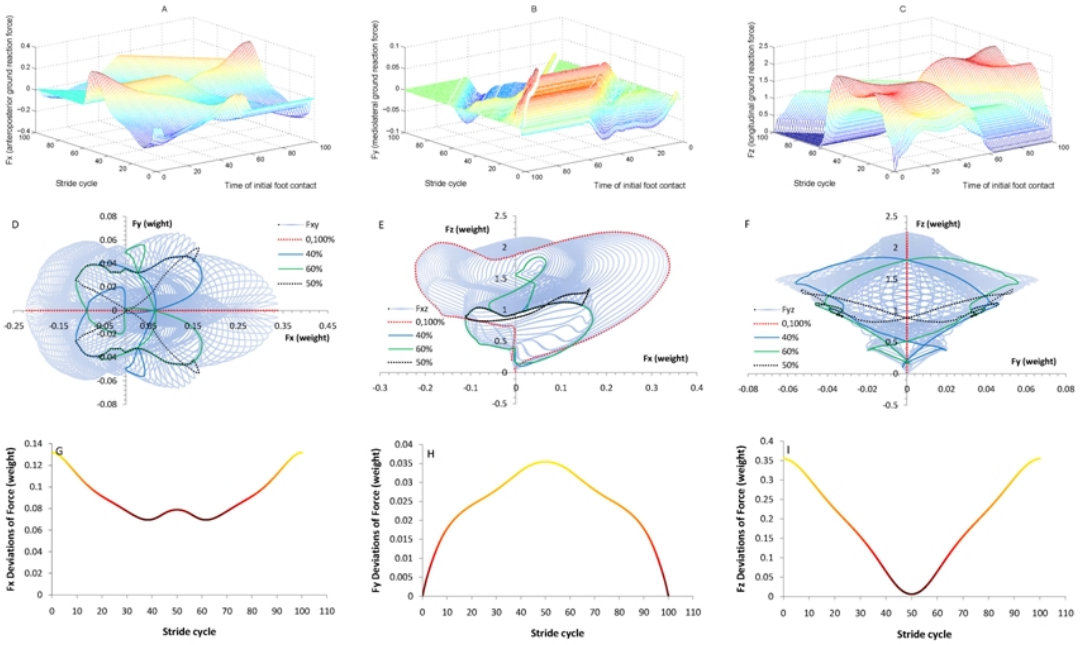

Fig. 1. Schematic illustration of the observed spectrum for tIFC and GRF showing the relationship between tIFC and GRF in three directions (Fig. 1A - C), together with tIFC and GRF resultant force in three planes (Fig. 1D - F), compared with a typical tIFC and dispersion of force correspondence (Fig. 1G - I)

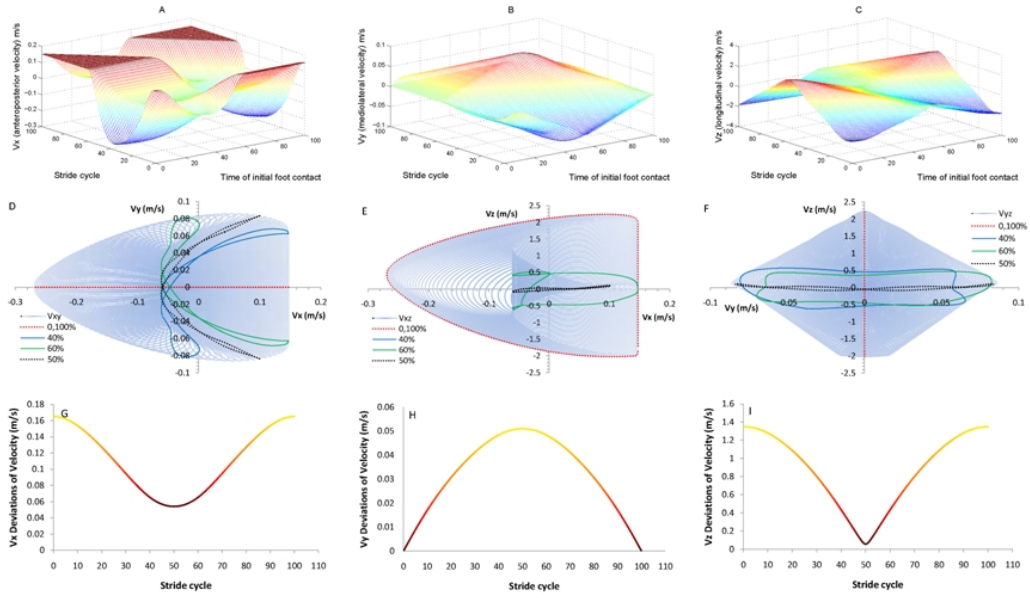

Fig. 2. Effective plots showing relationship between tIFC and COM velocity in three directions (Fig. 2A - C), tIFC and COM velocity in three planes (Fig. 2D - F) and tIFC and dispersion of COM velocity (Fig. 2G - I)

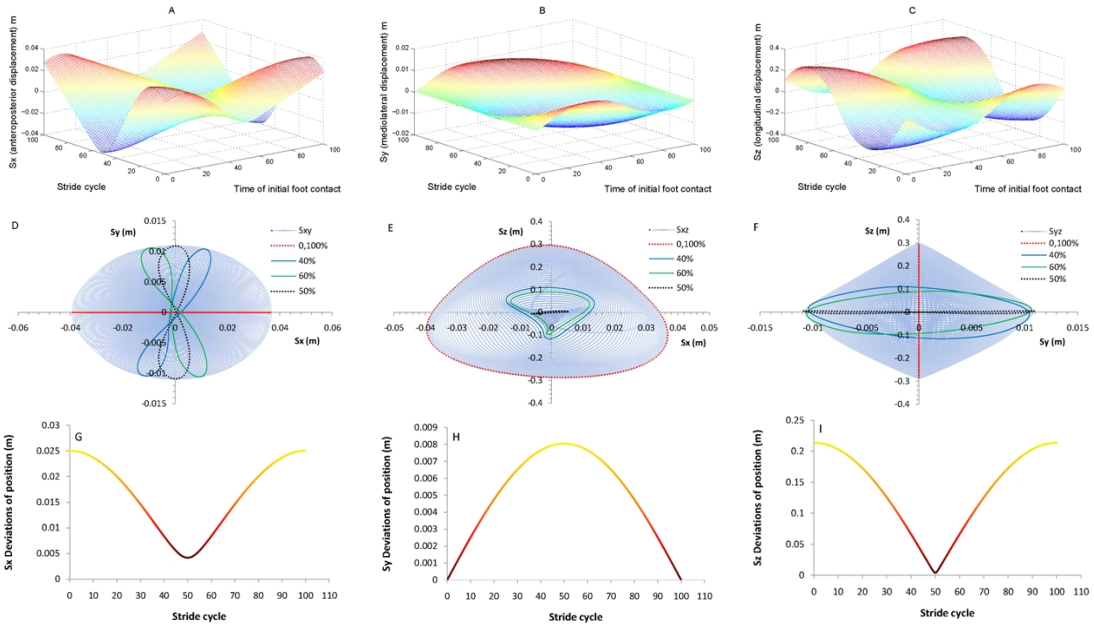

Fig. 3. COM displacement as a function of tIFC. The directional and planer components are shown in Fig. 3A - C and Fig. 3D - F, respectively. Fig. 3G - I shows the dispersion of COM displacement

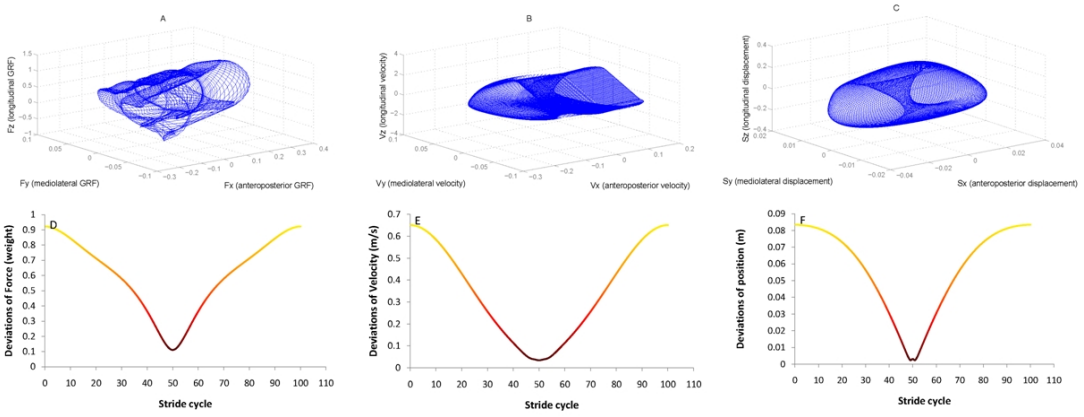

Fig. 4. Relationship between tIFC and dispersion of GRF, velocity and displacement of COM

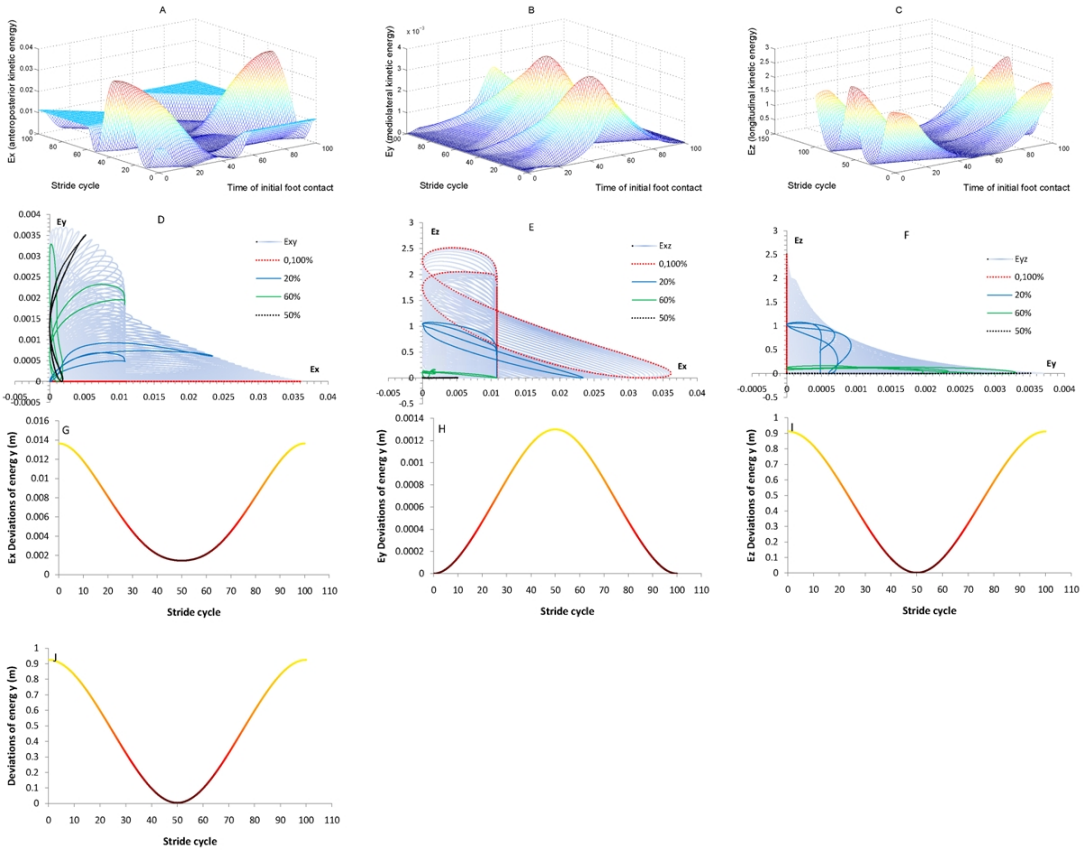

Fig. 5 Relationship between tIFC and kinetic energy. Fig. 5A - C tIFC and COM kinetic energy in three directions; Fig. 5D - F tIFC and COM kinetic energy in three planes; Fig. 5G - I tIFC and average kinetic energy

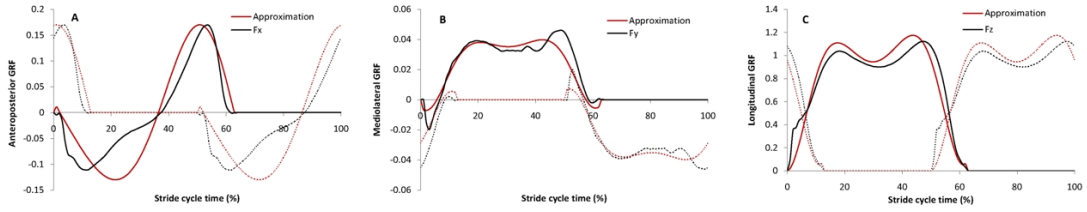

Fig. 6. GRF experimental results and Eq. 12. Fig. 6A Anteroposterior GRF and Eq. 12A. Fig. 6B Mediolateral GRF and Eq. 12B. Fig. 6C Vertical GRF and Eq. 12C

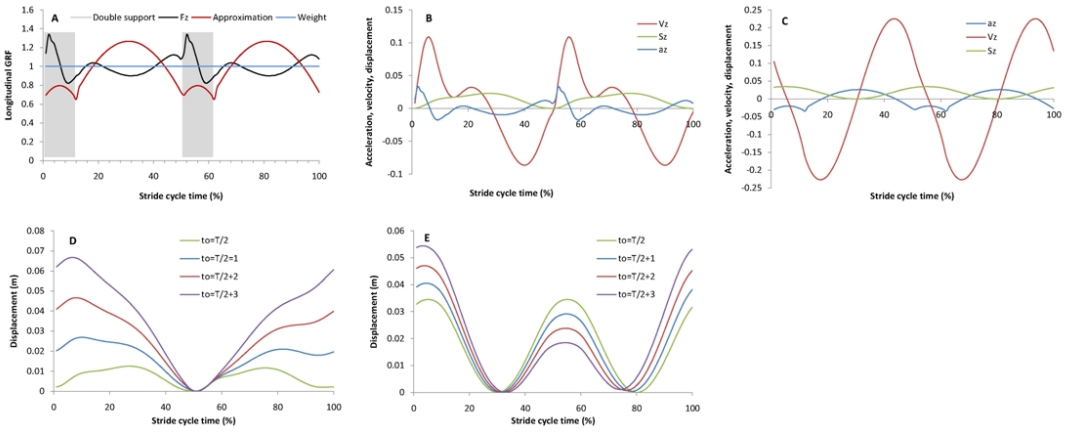

Fig. 7. Function simulation result and experimental result. Fig. 7A Comparison of vertical GRFs. Fig. 7B Kinematic quantity of COM calculated by approximation function of GRF (the acceleration was reduced 100-fold). Fig. 7C Kinematic quantity of COM calculated by GRF from experiment (the acceleration was reduced 100-fold). Fig. 7D Effect of tIFC upon the displacement of COM calculated by approximation function GRF. Fig. 7E Effect of tIFC upon the displacement of COM calculated by GRF from experiment

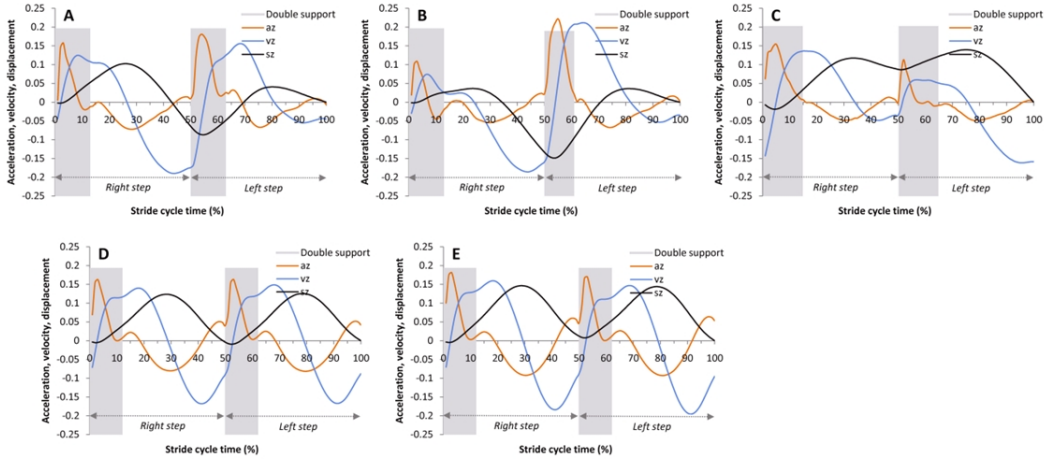

Fig. 8. Kinematic characteristics of COM in the vertical direction. Fig. 8A Kinematic characteristics of COM while walking from patients who had hemiarthroplasty. Fig. 8B Kinematic characteristics of COM while walking from patients who had Achilles tendon rupture. Fig. 8C Kinematic characteristics of COM while walking from patients who had rheumatoid arthritis. Fig. 8D Kinematic characteristics of COM while walking from healthy young men. Fig. 8E Kinematic characteristics of COM while walking from healthy young women. Information about the patients: patient with hemiarthroplasty: male; age: 57 years old; height: 178cm; weight: 82kg; with left hemiarthroplasty; test conducted 15 months after the surgery. Patient with Achilles tendon rupture: male; age: 48 years old; height: 167cm, weight: 75kg, with right foot Achilles tendon rupture when playing basketball; test conducted 13 months after the surgery. Patient with

rheumatoid arthritis: male; age: 68 years old; height: 166cm; weight: 78kg; still in treatment. The healthy young adults' data were adopted from literature [10]. The test was conducted with Zebris FDM System Gait Analysis. To make this figure more attractive, we multiplied acceleration values by 4, and displacement values by 5. The vertical GRF data were filtered with a cutoff frequency of 100Hz. The instants of touchdown and takeoff from the force plate were defined as when the vertical GRF first rose above 5N (touchdown) and reduced to 5N (takeoff)

5. CONCLUSION

In periodic motion, the foot's stance and swing substitute one another such that one foot always remains in stance. This allows the human body to be acted by the periodical GRF, which is related not only to the foot's movement style, but also to the substitution style of one foot with another. Following the biped movement style in normal gaits and the similar traits of GRF, we have been able to study the effect of tIFC upon the human COM dynamic characteristics based on the assumption that both feet's GRFs are the same in the same phase. Our results suggest that when tIFC falls in the middle of the other foot's stride cycle, the COM kinematics and dispersions of GRF acted on COM are the minimal, which has entailed the minimal average mechanical energy consumption of muscles. Our analysis suggests that it falls into the category of least-action principle and is consistent with the phenomenon that exists in normal gaits [10].

Based upon the least-action principle, we have observed that tIFC has caused the GRF and the COM regularities to form a closed-curve on the transverse and frontal plane, which might present a new method for gait evaluation. We advocate the use of this method to uncover and speed up the diagnosis simply by measuring the GRF for the patients with foot injuries or arthritis (for such patients, the model for these quantities is not symmetric [28]). Meanwhile, the patients need only walk a few steps in their normal gait, their COM dynamic characteristics will be acquired easily and more accurately. This is exactly what the clinic diagnosis is looking for. In addition to the human gait's adaptation to natural environment [20,29], the evolution of gait is the result of its observation of least-action principle. We believe that precise measurements of the variations of shear stress in natural gaits (bare-footed) shall profoundly enrich the content of least-action principle. A further study of least-action principle will be significant to the domains such as sport rehabilitation, biometric identification [30] and control of biped robot gaits [31,32].

ACKNOWLEDGMENTS

This project was funded by National Natural Science Foundation of China (http://www.nsfc.gov.cn) under the grant numbers of 10925208, 10972061 and 11172073 and by Guangdong Natural Science Foundation (http://gdsf.gdstc.gov.cn/) under the grant number of S2011010001829. The funders had no role in study design, data collection and analysis, decision to publish, or preparation of the manuscript. The authors would like to acknowledge the support from the subjects and the contributions from the editor and anonymous reviewers for their valuable comments and suggestions.

COMPETING INTERESTS

Authors have declared that no competing interests exist.

REFERENCES

1. Mitoma H, Hayashi R, Yanagisawa N, Tsukagoshi H. Characteristics of parkinsonian and ataxic gaits: a study using surface electromyograms, angular displacements and floor reaction forces. J Neurol Sci. 2000;174:22-39.
2. Kim CM, Eng JJ. Symmetry in vertical ground reaction force is accompanied by symmetry in temporal but not distance variables of gait in persons with stroke. Gait Posture. 2003;8:23-8.
3. Titianova EB, Tarkka IM. Asymmetry in walking performance and postural sway in patients with chronic unilateral cerebral infarction. J Rehabil Res Dev. 1995;32:236-44.
4. Biswasa A, Lemaire ED, Kofman J. Dynamic gait stability index based on plantar pressures and fuzzy logic. J Biomech. 2008;41:1574-81.
5. Wall JC, Turnbull GI. Gait asymmetries in residual hemiplegia. Arch Phys Med Rehabil. 1986;67:550-3.
6. Sadeghi H, Allard P, Prince F, Labelle H. Symmetry and limb dominance in able-bodied gait: a review. Gait Posture. 2000;12:34-45.
7. Kokshenev VB. Dynamics of human walking at steady speeds. Phys Rev Lett. 2004;93:208101-4.
8. Gutierrez-Farewik EM, Bartonek A, Saraste H. Comparison and evaluation of two common methods to measure center of mass displacement in three dimensions during gait. Hum. Movement Sci. 2006;25:238-56.
9. Murray MP. Gait as a total pattern of movement. Am J Phys Med. 1967;46: 290-333.
10. Fan YF, Loan M, Fan YB, Li ZY, Luo DL. Least-action principle in gait. Europhys Lett. 2009;87:58003.
11. Gard SA, Miff SC, Kuo AD. Comparison of kinematic and kinetic methods for computing the vertical motion of the body center of mass during walking. Hum Movement Sci. 2004;22: 597-610.
12. Winiarski S, Rutkowska-Kucharska A. Estimated ground reaction force in normal and pathological gait. Acta Bioeng Biomech. 2009;11:53-60.
13. Ren L, Jones RK, Howard D. Whole body inverse dynamics over a complete gait cycle based only on measured kinematics. J Biomech. 2008;41:2750-9.
14. Anderson FC, Pandy MG. Dynamic optimization of human walking. J Biomech Eng. 2001;123:381-90.
15. Chau T. A review of analytical techniques for gait data. Part 1: fuzzy, statistical and fractal methods. Gait Posture 2001;13: 49-66.
16. Cavagna GA. Force platforms as ergometers. J Appl Physiol. 1975;39:174-9.
17. Cavagna GA, Franzetti P, Fuchimoto T. The mechanics of walking in children. J Physiol. (London) 1983;343:323-39.
18. Donelan JM, Kram R, Kuo AD. Simultaneous positive and negative external mechanical work in human walking. J Biomech. 2002;35:117-24.
19. Marion JB, editor. Classical dynamics of particles and system. 2nd ed. Academic Press, Inc. New York; 1970.
20. Jenkins FA. Chimpanzee bipedalism: cineradiographic analysis and implications for evolution of gait. Science. 1972;178:877-9.
21. Srinivasan M, Ruina A. Computer optimization of a minimal biped model discovers walking and running. Nature. 2006;439:72-5.
22. Andriacchi TP, Ogle JA, Galante JO. Walking speed as a basis for normal and abnormal gait measurements. J Biomech. 1977;10: 261-8.
23. Jian Y, Winter DA, Ishac MG, Gilchrist L. Trajectory of the body COG and COP during initiation and termination of gait. Gait Posture 1993;1:9-22.
24. Riener R, Rabuffetti M, Frigo C. Stair ascent and descent at different inclinations. Gait

Posture. 2002;15:32-44.
25. Cavagna GA, Heglund NC, Taylor CR. Mechanical work in terrestrial locomotion: two basic mechanisms for minimizing energy expenditure. Am J Physiol. 1977;233:R243-R61.
26. Alexander RMN. Simple models of human movement. Appl Mech Rev. 1995;48:461–9.
27. Kuo AD. Energetics of actively powered locomotion using the simplest walking model. J Biomech Eng. 2002;124:113-20.
28. KFC. Technology Review; 2009.
Available: http://www.technologyreview.com/blog/arxiv/23569.
29. Richmond BG, Jungers WL. (Orrorin tugenensis femoral morphology and the evolution of hominin bipedalism. Science. 2008;319:1662-5.
30. Boulgouris NV, Hatzinakos D, Plataniotis KN. Gait recognition: A challenging signal processing technology for biometric identification. IEEE Signal Processing Mag. 2005;22:78-90.
31. Collins SH, Kuo AD. Recycling energy to restore impaired ankle function during human walking. PLos One. 2010;5:e9307
32. Ohgane K, Ueda KI. Instability-induced hierarchy in bipedal locomotion. Phys Rev E 2008;77:051915-27.

Peer-review history:
The peer review history for this paper can be accessed here:
http://www.sciencedomain.org/review-history.php?iid=243&id=11&aid=1852